Research Paper

Helium broadened propane absorption cross sections in the far-IR

A. Wong [a,*], B. Billinghurst [b], P.F. Bernath [a]

[a] *Department of Chemistry and Biochemistry, Old Dominion University, VA, USA, 23529*
[b] *Canadian Light Source Far-Infrared Beamline, 44 Innovation Blvd, Saskatoon, Canada SK S7N 2V3*

A B S T R A C T

Infrared absorption spectra for pure and He broadened propane have been recorded in the far-IR region (650-1300 cm^{-1}) at the Canadian Light Source (CLS) facility using either the synchrotron or internal glowbar source depending on the required resolution. The measurements were made for 4 temperatures in the range 202–292 K and for 3 pressures of He broadening gas up to 100 Torr. Infrared absorption cross sections are derived from the spectra and the integrated cross sections are within 10 % of the corresponding values from the Pacific Northwest National Laboratory (PNNL) for all temperatures and pressures.

© 2017 Elsevier B.V. All rights reserved.

Introduction

High resolution Fourier transform infrared (FTIR) spectroscopy is one of the most commonly used techniques for determining accurate molecular constants of gaseous molecules. These constants are used to generate line lists which can be applied to many atmospheric and planetary models, allowing for better interpretation of spectra and quantification of different species in various environments. Although this technique provides very accurate spectroscopic data, one major drawback is the increase in spectral congestion and complexity as the number of atoms in a molecule increases. One such molecule is propane.

Possessing 11 atoms and a C_{2v} equilibrium symmetry, propane has 27 fundamental vibrational modes; 7 of which lie below 1000 cm^{-1} in energy. These low energy states give rise to many hot bands that have appreciable intensity at warm (and even cold) temperatures which add to the line density of high resolution spectra and further complicates the analysis. As a result, there is a limited amount of accurate spectroscopic data of propane available: ν_9 (369 cm^{-1}) (Tchana et al., 2010), ν_{21} (921 cm^{-1}) (Perrin et al., 2015), ν_{26} (745 cm^{-1}) and $2\nu_9$-ν_9 (370 cm^{-1}) (Flaud et al., 2010) have been rovibrationally analyzed. Using microwave and submillimeter wave techniques (Drouin et al., 2006), the two lowest frequency vibrational levels (torsional modes situated near 217 cm^{-1} and 265 cm^{-1} (Grant et al., 1970)) have also been analyzed.

Due to a lack of accurate spectroscopic data, it is difficult to directly quantify and model propane in planetary atmospheres and this leads to inaccuracies when reporting atmospheric compositions. To help alleviate this issue, absorption cross-sections can be used in place of molecular constants. As absorption cross-sections are only dependent on the physical conditions of an experiment such as pressure and temperature, there is no need to analyze complex spectra in order to obtain accurate molecular constants. This becomes particularly important when interpreting spectra of gas giants such as Saturn, where propane has been detected (Guerlet et al., 2009).

Absorption cross sections of propane have previously been recorded mainly using two techniques: He-Ne laser spectroscopy and Fourier transform infrared (FTIR) spectroscopy. Because of the overlap between He-Ne laser line at 3.39 μm and the C-H stretching bands of propane in the 3 μm region (Jaynes & Beam, 1969), it is possible to monitor propane in combustion environments at elevated temperatures (Klingbeil et al., 2006; Mével et al., 2012; Yoshiyama et al., 1996). FTIR spectroscopy has been used to measure absorption cross sections of propane under conditions that are relevant to brown dwarfs and hot Jupiters (Beale et al., 2016), as well as the atmospheres of Earth and Titan (Sung et al., 2013). Databases such as GEISA (Jacquinet-Husson et al., 2016) and HITRAN (Rothman et al., 2013) also contain spectroscopic data for propane, however they are more relevant to Earth rather than giant planets.

Given that the dominant gases on Jupiter and Saturn are H_2 and He, it is necessary to obtain absorption cross sections of propane that are broadened by the appropriate gases at the correct temperatures and pressures. By doing so, this allows for direct comparison between laboratory measurements and those recorded from passing satellites.

Previously, we have reported absorption cross sections of pure and H_2 broadened propane between 200-298 K in the far-IR (FIR) region (600-1200 cm^{-1}) (Wong et al., 2017). These works are part of a larger research project which explores a range of small hydrocarbons that are found in cold planetary atmospheres, such as ethane (Hargreaves et al., 2015). The chosen temperatures correspond to the observed temperatures in different regions and altitudes of both Jupiter's and Saturn's atmosphere (e.g. the auroral regions of Jupiter (Sinclair et al., 2017)). Here, we present absorption cross sections of pure and He broadened propane within the same region and temperature regime as our previous work. Helium broadening parameters can be extracted from these data can then be used in radiative transfer models which would also incorporate hydrogen broadening. In an upcoming study, absorption cross sections of pure and broadened propane (with either H_2 or He) will be obtained from spectra recorded at temperatures as low as 150 K.

Experimental

Spectra of pure and He broadened propane were recorded at the Canadian Light Source (CLS) Far Infrared beamline using a White-type multipass cell set to 8 m (base length of two meters) (Johns et al., 1993; McKellar & Billinghurst 2015a, 2015b)) with a Bruker IFS 125 HR spectrometer. The spectrometer was fitted with a KBr beamsplitter, a liquid He cooled Ge: Cu bolometer and used either the external synchrotron radiation or the internal glowbar source. A NESLAB ULT-80DD refrigerated re-circulating methanol bath was used to cool the cell from ambient temperature (292 K) down to about 200 K. The cell temperature was monitored with 4 wire PT100 RTD sensors and left to equilibrate at each desired temperature. This reduced the temperature gradient across the cell and fluctuations during a measurement. Four temperatures were used: 202 K, 232 K, 261 K and 292 K. The recorded resolution was adjusted depending on the observed full-width at half-maximum (FWHM) of unblended lines (columns 4 and 5 in Table 1) to maximize scan efficiency and signal-to-noise levels.

Samples involving pure propane were introduced into the cell and monitored using a 10 Torr (1.33 kPa) Baratron pressure gauge. The accuracy of this pressure gauge is estimated to be ± 0.003 Torr. The pressure used was high enough such that the intensity of the ν_{26} band (centered near 750 cm^{-1}) remained below saturation. For propane-He mixtures, the cell was pre-filled with a small amount of propane before back-filling the desired amount of He specified in Table 1. A second Baratron pressure gauge (100 Torr, 13.3 kPa) monitored these higher pressures. In addition to the pure propane sample, three He-broadened spectra were recorded with total pressures (propane plus added He) of 1.066 kPa (8 Torr), 4 kPa (30 Torr) and 13.33 kPa (100 Torr).

For each set of experimental conditions (16 in total), background scans were recorded before and after each sample measurement. Pairs of forward and backward interferograms were recorded and Fourier transformed using a Blackman-Harris 3-Term apodization function and a zero-fill factor of 2. Single channel profiles were then post zero-filled with an additional factor of 4 to provide more accurate line positions and intensities. Individual files were averaged together and the final transmission spectrum was obtained by dividing the sample measurement with the most appropriate background measurement.

Results and discussion

Calibration

Absorption cross sections were obtained from the Pacific Northwest National Laboratory (PNNL) database (Sharpe et al., 2004) that were recorded at three temperatures: 278 K, 298 K and 323 K.

Table 1
Summary of P and P$_{\text{eff}}$ values for each experiment with corresponding FWHM of unblended lines near 700 cm^{-1}.

Pure

T (K)	P (Pa)	Peff[a] (Pa)	FWHM[b] (cm^{-1})	Resolution (cm^{-1})	
				Sample	Background
232.05	32.00	31.86	ca. 0.002	0.00096	0.001536
261.15	40.53	41.97			
292.34	46.00	39.52			

1.066 kPa total pressure

T (K)	P (Pa)	Peff[a] (Pa)	FWHM[b] (cm^{-1})	Resolution (cm^{-1})	
				Sample	Background
202.05	26.80	26.28	ca. 0.010	0.005	0.04
232.25	30.93	29.88			
261.35	59.06	56.78			
292.15	72.79	74.50			

4 kPa total pressure

T (K)	P (Pa)	Peff[a] (Pa)	FWHM[b] (cm^{-1})	Resolution (cm^{-1})	
				Sample	Background
202.35	75.73	74.09	ca. 0.029	0.01	0.04
232.25	106.66	114.54			
261.25	104.79	97.35			
292.25	115.72	114.04			

13.33 kPa total pressure

T (K)	P (Pa)	Peff[a] (Pa)	FWHM[b] (cm^{-1})	Resolution (cm^{-1})	
				Sample	Background
201.85	159.99	165.08	ca. 0.096	0.04	0.04
231.15	159.99	168.54			
261.35	146.79	148.66			
292.15	173.72	171.50			

[a] Effective pressures after calibration using PNNL cross sections (see text).
[b] Linewidths were measured using spectra recorded at 200 K, giving the narrowest FWHM.

Since the cross sections have units of ppm^{-1} m^{-1}, it is necessary to convert them to the appropriate units (cm^2 molecule^{-1}) by multiplying the absorption cross section with a factor, $F = 9.28697 \times 10^{-16}$ (Eq. 1),

$$F = \frac{k_B \times T \times \ln(10) \times 10^4}{0.101325} \qquad (1)$$

where T = 296 K. The integrated cross section values can then be determined by integrating over the desired spectral range. It is possible to integrate across the entire spectral range (i.e. 600-1200 cm^{-1}), however there is some noticeable variation in the baseline level of each absorption cross section which affects the determined values: 7.716×10^{-19}, 9.641×10^{-19} and 9.137×10^{-19} cm molecule^{-1} at 278 K, 298 K and 323 K respectively, are obtained. As a consequence, there was a need to restrict the lower and upper integration limits, to 680 and 970 cm^{-1} respectively, in order to minimize the influence of the baseline. Furthermore, only the absorption cross section recorded at 298 K was used as it had the flattest baseline within the chosen integration limits.

Cross sections and calibration

An absorption cross section can be obtained from a transmission spectrum using Eq. 2 (Harrison & Bernath, 2010):

$$\sigma(\nu, T) = -\xi \frac{10^4 k_B T}{Pl} \ln \tau(\nu, T) \qquad (2)$$

where $\sigma(\nu, T)$ is the absorption cross section (cm^2 molecule^{-1}). k_B is the Boltzmann constant (J K^{-1}), P is the pressure (Pa), l is the op-
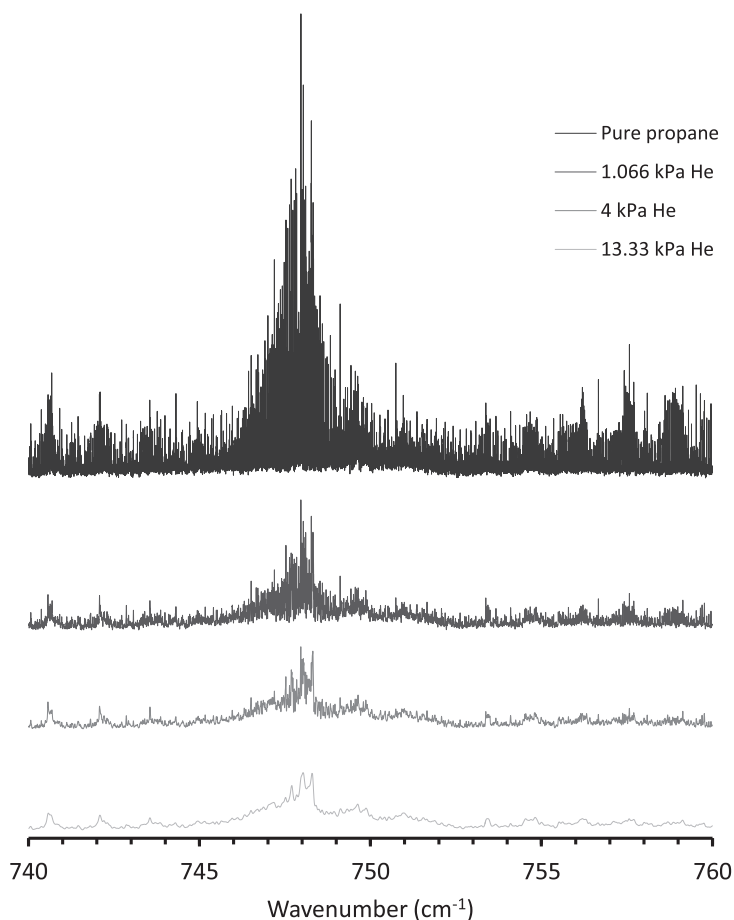
Fig. 1. Vertically offset absorption cross sections of propane, at 292 K, with increasing pressures of He.

tical path length (m), T is the temperature (K) and τ is the transmission as a function of wavelength (cm^{-1}) and temperature (K). ξ is used as a calibration factor to account for any difficulties in accurately determining the pressure-pathlength of the absorbing gas.

Since the absorption cross section is already in the appropriate units (cm^2 molecule^{-1}), it is possible to directly integrate over the same frequency range as before to determine the integrated cross sections.

Ideally, the integrated cross sections from CLS and PNNL should be equal ($\int_{970cm^{-1}}^{680cm^{-1}} \sigma_{CLS} d\nu = \int_{970cm^{-1}}^{680cm^{-1}} \sigma_{PNNL} d\nu$). However, in practice, differences between these values can be observed and therefore ξ is used as a calibration factor. This results in new P_{eff} values (column three in each of the tables in Table 1) such that the CLS integrated cross sections would be equal to the PNNL values. The obtained cross sections corresponding to each experimental condition listed in Table 1 are given as part of the supplementary material. The agreement between the two pressures is satisfactory and in the end, we decided to use the measured pressures and set the calibration factor ξ to 1.

Pressure broadening

Fig. 1 demonstrates pressure induced broadening at 292 K as the amount of He introduced into the system is increased. Spectral features in the absorption cross sections for pure propane initially appear as intense and generally well resolved rotational-vibrational lines. As the quantity of He is increased, individual lines decrease in intensity, broaden and overlap with each other to create a pseudo-continuum. Although the band intensity changes as the foreign gas pressure is increased, the integrated area itself is retained due to the observed pseudo-continuum.

Since the calculated integrated cross section values remain consistent across all temperature and pressure ranges and are within 10 % of the PNNL value, this shows that the recorded T and P values are indeed correct and accurate. Results for the measurement of pure propane at 200 K is not included because the transmission spectrum showed visible signs of contamination on the cell mirrors.

Conclusions

High resolution transmission spectra of pure and He broadened propane have been recorded at the CLS facility. Spectra were recorded within the FIR region (600-1250 cm^{-1}) at temperatures (200-298 K) and pressures suitable for planetary atmospheres. Absorption cross sections were obtained from transmission spectra. Helium has been used as the foreign broadening gas corresponding to the second most abundant molecule on Jupiter and Saturn. For the analysis of planetary spectra, the He broadened cross sections can be combined with our previous H$_2$ broadened data (Wong et al., 2017) and interpolated to any temperature and pressure in the measurement range.

In the absence of accurate molecular constants and line parameters from high resolution analyses, cross sections are a convenient means of providing accurate spectroscopic data which can be used to interpret spectra, quantify species and model planetary environments. Furthermore, absorption cross sections do not require analysis of highly complex rotation-vibration spectra and are directly relatable to observations.

Synchrotron radiation was used for transmission spectra recorded at the highest resolution. The highly collimated nature of the beam generates FIR radiation that has a higher flux and signal-to-noise level in comparison to conventional benchtop sources. The internal glowbar source was used for lower resolution experiments where the numerical aperture was increased and the synchrotron advantage was lost.

Acknowledgements

Supplementary materials

Supplementary material associated with this article can be found, in the online version, at doi:10.1016/j.molap.2017.06.003.

References

Beale, C.A., Hargreaves, R.J., Bernath, P.F., 2016. J. Quant. Spectrosc. Radiat. Transfer 182, 219–224.
Drouin, B.J., Pearson, J.C., Walters, A., Lattanzi, V., 2006. J. Mol. Spectrosc. 240, 227–237.
Flaud, J.-M., Tchana, F.K., Lafferty, W.J., Nixon, C.A., 2010. Mol. Phys. 108, 699–704.
Grant, D.M., Pubmire, R.J., Livingston, R.C., Strong, K.A., McMurray, H.L., Brugger, R.M., 1970. J. Chem. Phys. 52, 4424–4436.
Guerlet, S., Fouchet, T., Bézard, B., Simon-Miller, A.A., Flasar, F.M., 2009. Icarus 203, 214–232.
Hargreaves, R.J., Bernath, P.F., Appadoo, D.R.T., 2015. J. Mol. Spectrosc. 315, 102–106.
Harrison, J.J., Bernath, P.F., 2010. J. Quant. Spectrosc. Radiat. Transfer 111, 1282–1288.
Jacquinet-Husson, N., Armante, R., Scott, N.A., Chédin, A., Crépeau, L., Boutammine, C., 2016. J. Mol. Spectrosc. 327, 31–72.
Jaynes, D.N., Beam, B.H., 1969. Appl. Opt. 8, 1741–1742.
Johns, J.W.C., Lu, Z., McKellar, A.R.W., 1993. J. Mol. Spectrosc. 159, 210–216.
Klingbeil, A.E., Jeffries, J.B., Hanson, R.K., 2006. Meas. Sci. Technol. 16, 1950–1957.
McKellar, A.R.W., Billinghurst, B.E., 2015a. J. Mol. Spectrosc. 315, 24–29.
McKellar, A.R.W., Billinghurst, B.E., 2015b. J. Mol. Spectrosc. 315, 41–45.
Mével, R., Boettcher, P.A., Shepherd, J.E., 2012. Chem. Phys. Lett. 531, 22–27.
Perrin, A., Tchana, F.K., Flaud, J.-M., Manceron, L., Demaison, J., Vogt, M., Groner, P., Lafferty, W.J., 2015. J. Mol. Spectrosc. 315, 55–62.
Rothman, L.S., Gordan, I.E., Babikov, Y., Barbe, A., Benner, D.C., Bernath, P.F., Birk, M., Bizzocchi, L., Boudon, V., Brown, L.R., Campargue, A., Chance, K., Cohen, E.A., Coudert, L.H., Devi, V.M., Drouin, B.J., Fayt, A., Flaud, J.-M., Gamache, R.R., Harrison, J.J., Harmann, J.-M., Hill, C., Hodges, J.T., Hacquemart, D., Jolly, A., Lamouroux, J., Le Roy, R.J., Li, G., Long, D.A., Lyulin, O.M., Mackie, C.J., Massie, S.T., Mikhailenko, S., Müller, H.S.P., Naumenko, O.V., Nikitin, A.V., Orphal, J., Perevalov, V., Perrin, A., Polovtseva, E.R., Richard, C., Smith, M.A.H., Starikova, E., Sung, K., Tashkun, S., Tennyson, J., Toon, G.C., Tyuterev, Vl.G., Wagner, G., 2013. J. Quant. Spectrosc. Radiat. Transfer 130, 4–50.
Sharpe, S.W., Johnson, T.J., Sams, R.L., Chu, P.M., Rhoderick, G.C., Johnson, P.A., 2004. Appl. Spectrosc. 58, 1452–1461.
Sinclair, J.A., Orton, G.S., Greathouse, T.K., Fletcher, L.N., Moses, J.I., Hue, V., Irwin, P.G.J., 2017. Icarus 292, 182–207.
Sung, K., Toon, G.C., Mantz, A.W., Smith, M.A.H., 2013. Icarus 226, 1499–1513.
Tchana, F.K., Flaud, J.-M., Lafferty, W.J., Manceron, L., Roy, P., 2010. J. Quant. Spectrosc. Radiat. Transer 111, 1277–1281.
Wong, A., Hargreaves, R.J., Billinghurst, B., Bernath, P.F., 2017. J. Quant. Spectrosc. Radiat. Transfer 198, 141–144.
Yoshiyama, S., Hamamoto, Y., Tomita, E., Minami, K., 1996. JSAE Rev. 17, 339–345.